An Initial Assessment of Antarctic Sea Ice Extent in the CMIP5 Models

JOHN TURNER, THOMAS J. BRACEGIRDLE, TONY PHILLIPS, GARETH J. MARSHALL, AND J. SCOTT HOSKING

British Antarctic Survey, Natural Environment Research Council, Cambridge, United Kingdom

(Manuscript received 20 January 2012, in final form 9 August 2012)

ABSTRACT

This paper examines the annual cycle and trends in Antarctic sea ice extent (SIE) for 18 models used in phase 5 of the Coupled Model Intercomparison Project (CMIP5) that were run with historical forcing for the 1850s to 2005. Many of the models have an annual SIE cycle that differs markedly from that observed over the last 30 years. The majority of models have too small of an SIE at the minimum in February, while several of the models have less than two-thirds of the observed SIE at the September maximum. In contrast to the satellite data, which exhibit a slight increase in SIE, the mean SIE of the models over 1979–2005 shows a decrease in each month, with the greatest multimodel mean percentage monthly decline of 13.6% decade^{-1} in February and the greatest absolute loss of ice of -0.40×10^6 km^2 decade^{-1} in September. The models have very large differences in SIE over 1860–2005. Most of the control runs have statistically significant trends in SIE over their full time span, and all of the models have a negative trend in SIE since the mid-nineteenth century. The negative SIE trends in most of the model runs over 1979–2005 are a continuation of an earlier decline, suggesting that the processes responsible for the observed increase over the last 30 years are not being simulated correctly.

1. Introduction

Since the late 1970s sea ice extent (SIE) around the Antarctic continent has increased at a statistically significant rate (Comiso and Nishio 2008; Turner et al. 2009; Zwally et al. 2002). This is in marked contrast to the ice conditions over the Arctic Ocean, where there has been a sharp decline over the same period (Stroeve et al. 2007). The reasons for the overall increase in Antarctic SIE over the last 30 years are still under debate. Turner et al. (2009) carried out model experiments that suggested that the loss of stratospheric ozone had played a significant role through deepening the Amundsen Sea low, resulting in greater southerly flow over the Ross Sea, which has experienced a large increase in ice cover. However, the model experiments of Sigmond and Fyfe (2010) gave a year-round *decrease* of ice when stratospheric ozone was reduced, suggesting that the increase is likely caused by processes not linked to stratospheric ozone depletion. A possible role for the ocean in the increase of ice was proposed by Zhang (2007).

The simulation of sea ice variability presents a number of problems for climate models. Small errors in oceanic or atmospheric conditions can lead to errors in the SIE, ice thickness, or speed of sea ice drift (McLaren et al. 2006). Errors in model bathymetry (Turner et al. 2001) and even errors in the representation of the tropical atmosphere can result in sea ice biases around the Antarctic continent (Song et al. 2011). The Coupled Model Intercomparison Project (CMIP) of the World Climate Research Programme (WCRP) comprises a collection of contemporary coupled atmosphere–ocean climate models and offers a means to assess our ability to simulate correctly the trends and variability of sea ice. The sea ice data from phase 3 of CMIP (CMIP3), which were used in the Intergovernmental Panel on Climate Change (IPCC) Fourth Assessment Report (AR4) were assessed by Arzel et al. (2006). They found that for the first 20 years of the satellite era the multimodel mean SIE agreed reasonably well with the satellite data in terms of SIE. However, at the sea ice maximum in September the multimodel mean had a decrease of Antarctic average SIE over this period while the satellite-derived extent had increased.

Phase 5 of CMIP (CMIP5) will provide the model output that will form the basis of the Fifth Assessment Report (AR5) of the IPCC. In this paper we present an

Corresponding author address: Prof. John Turner, British Antarctic Survey, Natural Environment Research Council, High Cross, Madingley Road, Cambridge CB3 0ET, United Kingdom.
E-mail: jtu@bas.ac.uk

DOI: 10.1175/JCLI-D-12-00068.1

TABLE 1. SIEs, variability, and trends in the satellite data and CMIP5 models. Further information on the models used can be obtained from http://esg-pcmdi.llnl.gov/internal/esg-data-node-documentation/cmip5_controlled_vocab.txt/view. Here, n/a indicates not applicable.

Model	Country	Period for which sea ice data are available	No. of ensemble members	Mean annual SIE (1979–2005) (10^6 km^2)	SD of mean annual SIE in the satellite data and model runs	SD of mean annual SIE between model runs (10^6 km^2)	Trend in mean annual SIE for 1979–2005 (percent per decade). The value in parentheses gives the value when the long-term trend from the control run has been removed. Note that control run trends are not available for HadCM3 and the GISS models.	RMS fit of the models' annual SIE cycle to the satellite data (10^6 km^2)
Beijing Climate Center Climate System Model, version 1 (BCC-CSM1.1)	China	1850–2012	3	13.0	1.24	0.0	−3.7 (−3.7)	1.8
Canadian Earth System Model, version 2 (CanESM2)	Canada	1850–2005	5	13.1	0.82	0.3	−5.0 (−5.0)	2.0
Community Climate System Model, version 4 (CCSM4)	USA	1850–2005	1	17.8	0.73	n/a	−4.1 (−4.1)	6.1
Centre National de Recherches Météorologiques Coupled Global Climate Model, version 5 (CNRM-CM5)	France	1850–2005	10	7.3	0.70	0.4	−6.8 (−6.7)	4.9
Commonwealth Scientific and Industrial Research Organisation Model, Mark 3.6.0 (CSIRO Mk3.6)	Australia	1850–2005	10	14.5	0.53	0.2	−1.5 (−1.4)	3.9
Goddard Institute for Space Studies (GISS) Model E2-H (GISS-E2-H)	USA	1850–2005	5	4.9	0.18	0.2	−1.8	7.5
GISS Model E2-R (GISS-E2-R)	USA	1850–2005	2	6.7	0.73	0.1	0.3	5.4
Third climate configuration of the Met Office Unified Model (HadCM3)	UK	1859–2005	10	13.6	0.58	0.1	−2.3	2.8
Hadley Centre Global Environmental Model, version 2 (HadGEM2) (Carbon Cycle) (HadGEM2-CC)	UK	1859–2005	1	9.1	0.62	n/a	−1.7 (−1.9)	3.3
HadGEM2 (Earth System) (HadGEM2-ES)	UK	1859–2005	1	9.8	0.64	n/a	−3.3 (−3.2)	2.6
Institute of Numerical Mathematics Coupled Model, version 4 (INM-CM4)	Russia	1850–2005	1	6.4	0.46	n/a	−6.3 (−6.4)	5.9
L'Institut Pierre-Simon Laplace Coupled Model, version 5A Low Resolution (IPSL-CM5A-LR)	France	1850–2005	4	9.2	0.64	0.2	−3.4 (−3.3)	3.6

TABLE 1. (*Continued*)

Model	Country	Period for which sea ice data are available	No. of ensemble members	Mean annual SIE (1979–2005) (10^6 km^2)	SD of mean annual SIE in the satellite data and model runs	SD of mean annual SIE between model runs (10^6 km^2)	Trend in mean annual SIE for 1979–2005 (percent per decade). The value in parentheses gives the value when the long-term trend from the control run has been removed. Note that control run trends are not available for HadCM3 and the GISS models.	RMS fit of the models' annual SIE cycle to the satellite data (10^6 km^2)
Model for Interdisciplinary Research on Climate (MIROC) Earth System Model with atmospheric chemistry (MIROC-ESM-CHEM)	Japan	1850–2005	1	13.5	0.41	n/a	−1.6 (−1.1)	2.2
MIROC Earth System Model (MIROC-ESM)	Japan	1850–2005	1	12.8	0.67	n/a	−4.6 (−4.0)	1.6
MIROC, version 4h (MIROC4h)	Japan	1950–2005	3	11.0	0.61	0.1	−5.8 (−5.4)	1.3
MIROC, version 5 (MIROC5)	Japan	1850–2005	1	3.3	0.20	n/a	−3.3 (−2.7)	9.2
Max Planck Institute Earth System Model low resolution (MPI-ESM-LR)	Germany	1850–2005	3	7.0	0.67	0.1	−1.9 (−1.9)	5.2
Meteorological Research Institute Coupled General Circulation Model, version 3 (MRI-CGCM3)	Japan	1850–2005	5	14.0	0.59	0.4	−2.3 (−2.3)	2.2
Norwegian Earth System Model, version 1-M (NorESM1-M)	Norway	1850–2005	3	12.7	0.57	0.2	−1.5 (−1.5)	0.9
Satellite	n/a	1979–2005	—	11.9	0.25	n/a	1.1	n/a

initial assessment of the SIE in the historical CMIP5 model runs encompassing the period 1979–2005. We also examine the Antarctic SIE in the long control runs of the models that were carried out with preindustrial forcing, which provided the initial conditions for the historical runs. We focus on the broadscale simulation of the Southern Ocean SIE using the data available on the CMIP5 web site. The results will be of value to the major climate modeling centers in detailed assessments of their own models.

We show that as with CMIP3 the models do not simulate the recent increase in Antarctic SIE observed in the satellite data. In fact, most of the model runs have a decrease in SIE in every month of the year, with the greatest percentage loss in late summer/early fall (February–April), a pattern of change very similar to that observed in the Arctic.

2. Data

The CMIP5 model monthly mean historical sea ice area fraction data were obtained from the web site of the Program for Climate Model Diagnostics and Intercomparison (PCMDI) (http://cmip-pcmdi.llnl.gov/cmip5/). Eventually around 40 coupled models will provide data for the CMIP5 initiative, but at the time of writing the 19 models listed in Table 1 have made data available, and it is these data that form the basis of this study (note that expansions of all model names are available in Table 1). For 18 of the models the historical runs cover the period from the mid-nineteenth century to 2005, with the MIROC4h run starting in 1950. In these runs the models were forced by observed changes in greenhouse gas and stratospheric ozone concentrations, aerosols, and solar variability. The number of ensemble members ranges from 1 to 10 (Table 1). For all the models except HadCM3 we also have the SIE data for the control runs that cover periods of between 100 and over 1000 years. These data give an indication of the stability of the Antarctic SIE in the models. For selected models we have also obtained the ocean temperature and salinity data to aid the investigation of the large biases that some models have in SIE.

We regridded the data from PCMDI onto a common 1.0° longitude by 0.5° latitude grid before performing the analysis. Model SIE was computed as the total area of all grid cells where sea ice area fraction exceeded 15%. Here we focus primarily on the period 1979–2005 since that overlaps with the available satellite record of SIE, which was obtained from the U.S.National Snow and Ice Data Center (ftp://sidads.colorado.edu/DATASETS/NOAA/G02135/). These fields are based on the sea ice index derived from the National Aeronautics and Space Administration (NASA) team algorithm.

3. The observed changes in SIE

For 1979–2005 the annual mean Antarctic SIE has increased at a rate of 126 949 km^2 decade^{-1} or 1.1% decade^{-1} (see Table 1), which is significant at $<5\%$ level. The trends were computed using a standard least squares method, with the methodology used to calculate the significance levels based upon Santer et al. (2000). Briefly, an effective sample size was calculated based on the lag-1 autocorrelation coefficient of the regression residuals. This effective sample size was used for the computation of the standard error and in indexing the critical values of Student's t distribution. The largest percentage SIE increases are observed during February–May, with the largest monthly increase in March (5.5% decade^{-1}), which is statistically significant at $<5\%$ level. Figure 1 shows that the overall Antarctic SIE has increased in every month of the year, although only three months have a significant trend [March (5%), April (10%), and May (5%)]. Since 2005 the increase of Antarctic SIE has continued, although we note that there are possible issues with merging satellite sea ice datasets for this period (Screen 2011). However, the trend in total Antarctic SIE masks large regional variations. Over the last 30 years sea ice has increased around much of the coast of East Antarctica but shown a contrasting change between the Antarctic Peninsula and the Ross Ice Shelf region, with a negative (positive) trend in the Amundsen–Bellingshausen Sea (Ross Sea) (Stammerjohn et al. 2008; Turner et al. 2009). The magnitudes of both these trends are large, but the greatest change has been in the Ross Sea so that there has been an overall increase in the SIE across the sector of the Southern Ocean between the Peninsula and the Ross Sea.

4. Simulation of sea ice by the CMIP5 models

Inspection of the model SIE data shows that the models have very different magnitudes for the mean February minimum (Fig. 2). CNRM-CM5 has the least sea ice in February of any of the models, with only 0.7% of the SIE observed in the satellite data (1979–2005). In a number of years this model has no ice at all around the Antarctic continent in this month, whereas in other years there is a small amount of ice over the western Weddell Sea. The MIROC5, INMCM4, GISS-E2-H, GISS-E2-R, and MPI-ESM-LR models have a little more ice over the western Weddell Sea in February, but virtually no ice anywhere else around the continent. With so little ice in February in these models the negative trends in the absolute amount of ice over 1979–2005 are consequently quite small, as there is not a great deal of ice to lose.

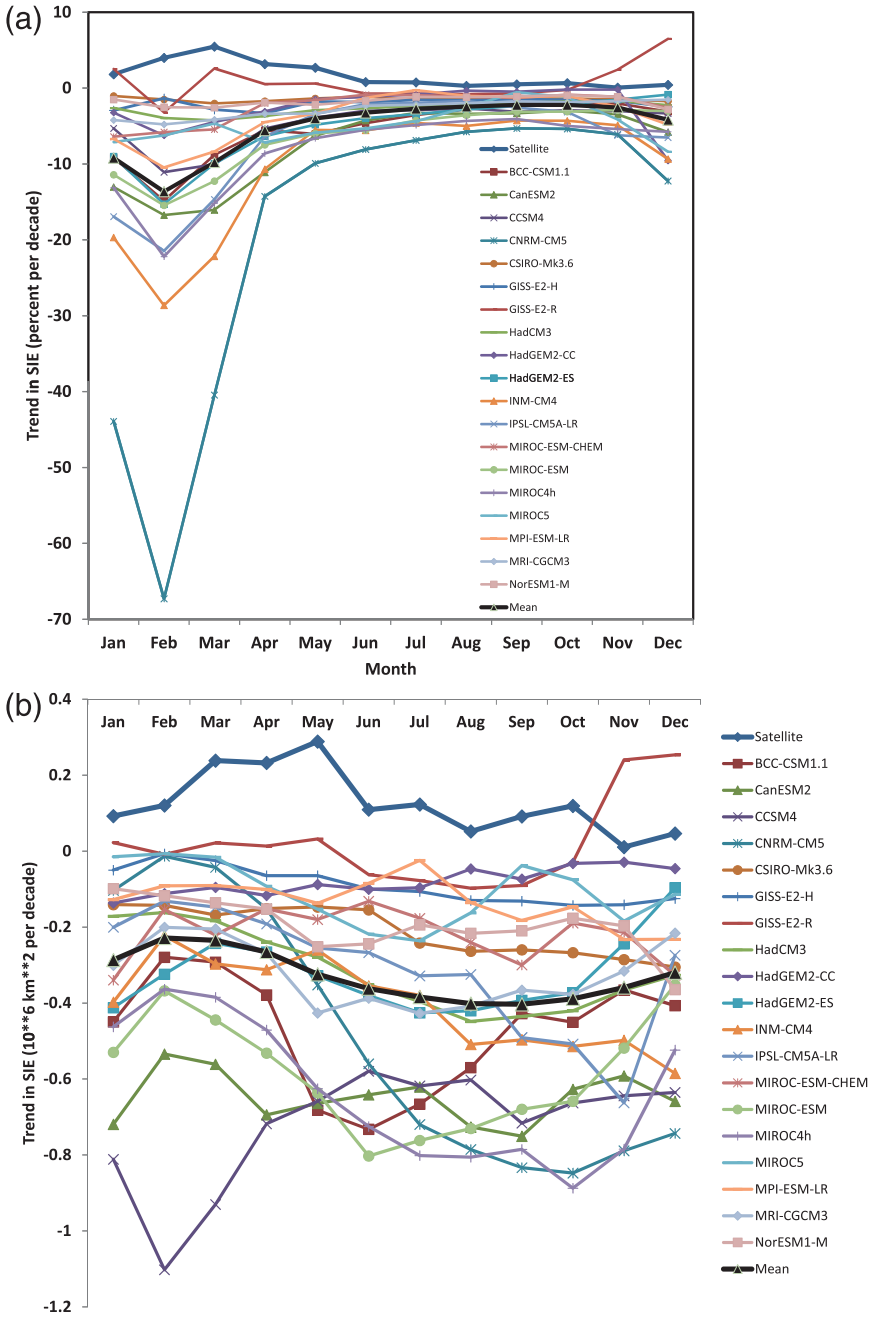

FIG. 1. Monthly trends of SIE from the satellite data (thick blue line) and CMIP5 models over 1979–2005. For models with more than one ensemble member the mean of the ensemble members is plotted. The mean of all the models is shown as a black line. Shown are (a) percentage trend per decade and (b) absolute trend per decade (10^6 km^2 decade^{-1}).

The 19 models have large differences in their mean annual cycle of SIE (Fig. 2). MIROC5 has the least ice throughout the year with only 36% of the observed SIE at the maximum in September. INMCM4, GISS-E2-R, and MPI-ESM-LR also have large negative errors in SIE over the year. Conversely, HadCM3 has a large positive bias in spring with the maximum a month later than observed in the satellite data, with the latter also applying to the two other Hadley Centre models. CanESM2, BCC-CSM1.1, MIROC-ESM, and MIROC-ESM-CHEM all do reasonably well at the ice minimum and during the winter growth phase, but have too much

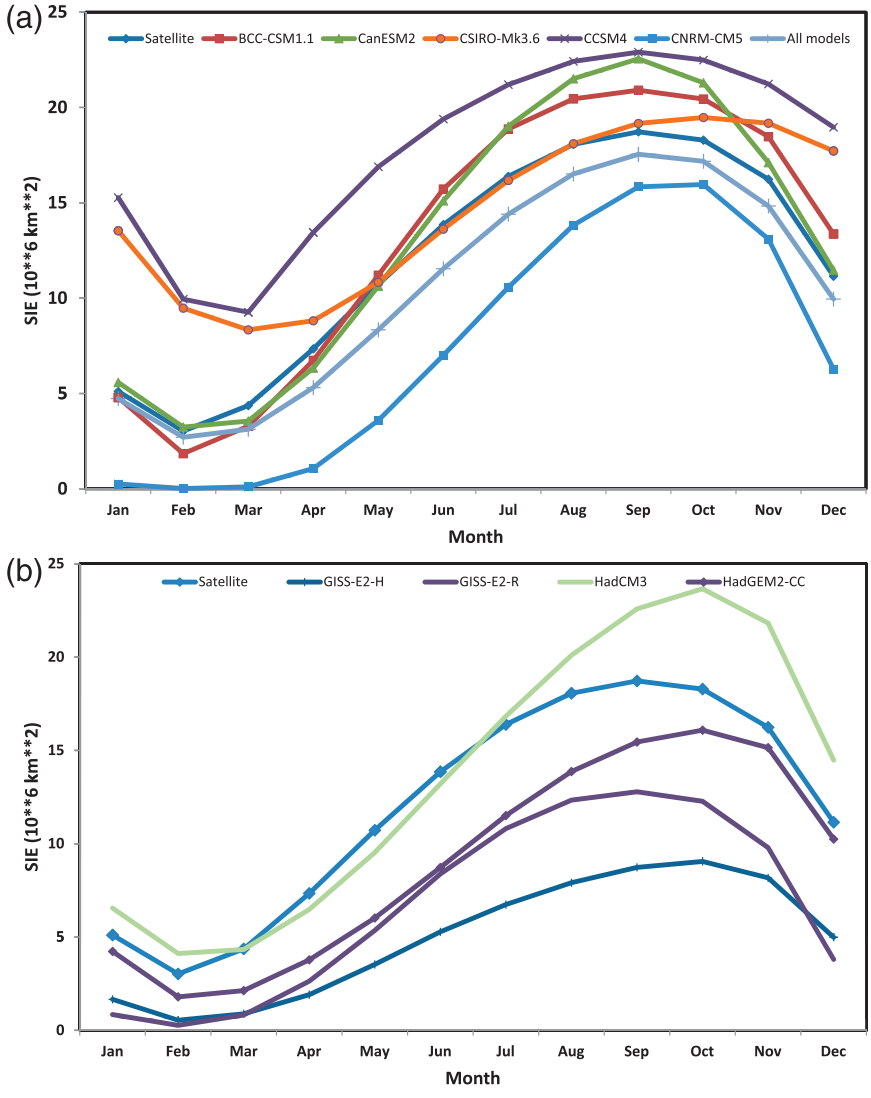

FIG. 2. The mean annual cycle (1979–2005) of SIE in the 19 CMIP5 models and the mean of all the models. For models with more than one ensemble member the mean of the ensemble members is plotted. The data are shown on four graphs for clarity. Each graph shows the annual cycle of SIE derived from the satellite data.

ice near the maximum. The RMS differences between modeled and observed annual SIE cycle are given in Table 1 and show that the NorESM1-M model has the best fit and the MIROC5 model the worst. The ensemble mean annual cycle of SIE from the 19 models has a negative bias compared to the satellite data throughout the year (Fig. 2). The magnitude of this negative bias increases from 0.3×10^6 km^2 in February to 1.2×10^6 km^2 in March and stays within the range 2.0×10^6–2.4×10^6 km^2 from April to July.

The 1979–2005 period examined here is at the end of long model integrations starting in the 1850s and it is instructive to examine how the SIEs evolved over the duration of the model runs. Figure 3 shows the February SIE since 1860 for all the model integrations. The striking feature is the very large differences in model SIE in the presatellite era, with the February mean extent over 1860–69 varying from 0.07×10^6 km^2 (CNRM-CM5) to 12.18×10^6 km^2 (CCSM4). The historical integrations are initialized from long control runs of each model and Fig. 3 shows that many of the models had large biases in their initial SIE close to the ice minimum. Some of the models, such as the two GISS models, CNRM-CM5, and MIROC5, have very large negative extent biases. The CSIRO-Mk3.6 and CCSM4 models have large positive biases (a factor of 3–4 compared to the

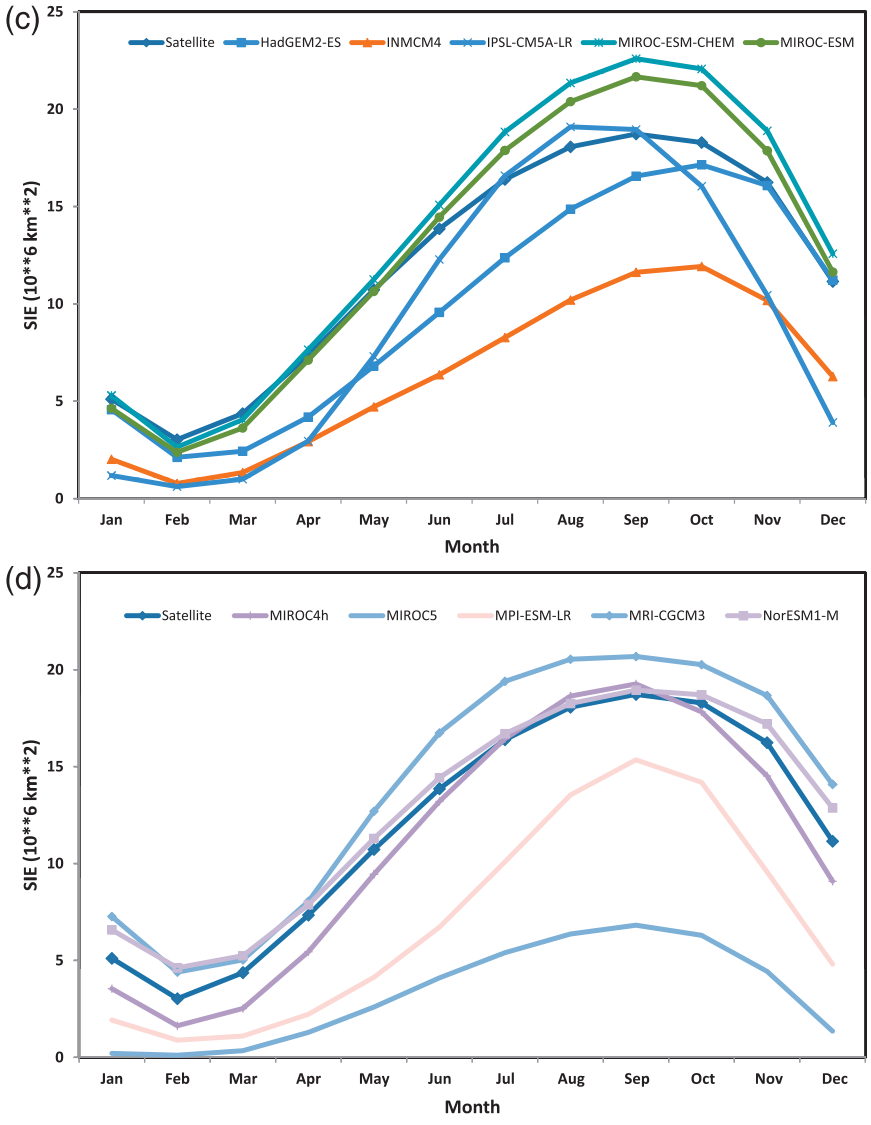

FIG. 2. (*Continued*)

satellite period) at this time of year. Examination of the ocean temperature data for the historical runs suggests that biases in the ocean play a part in the establishment of the SIE anomalies, but that other factors are also involved. For example, the CSIRO and HadCM3 models have ocean temperatures that are too cold at high southern latitudes, which is consistent with the positive SIE anomalies.

Figure 1 shows the trends for the 1979–2005 period of the historical runs of the 19 CMIP5 models by month. For each model the trend shown is an average of all available ensemble members. All the models except GISS-E2-R have a decrease in annual mean SIE (Table 1), with the mean of all the models being -3.2% decade^{-1} (-0.33×10^6 km^2 decade^{-1}). The mean of all the model trends has the largest percentage decrease of SIE in February (-13.6% decade^{-1}, -0.23×10^6 km^2 decade^{-1}; the median trend is -10.5% decade^{-1},) and 14 of the 19 models also have their largest percentage decrease in that month. However, it should be noted that the absolute amount of sea ice in February is small so that modest losses of ice can result in large percentage changes. A further three models have their largest percentage decline in March. Figure 1a shows that the models have a very large range of 27-yr percentage trends in the months of January to March, with February having the greatest intermodel spread in trend [standard deviation (SD) of 15.2% decade^{-1}]. The intermodel differences in percentage trend decrease rapidly after March with September having the smallest spread (SD of 1.3% decade^{-1}).

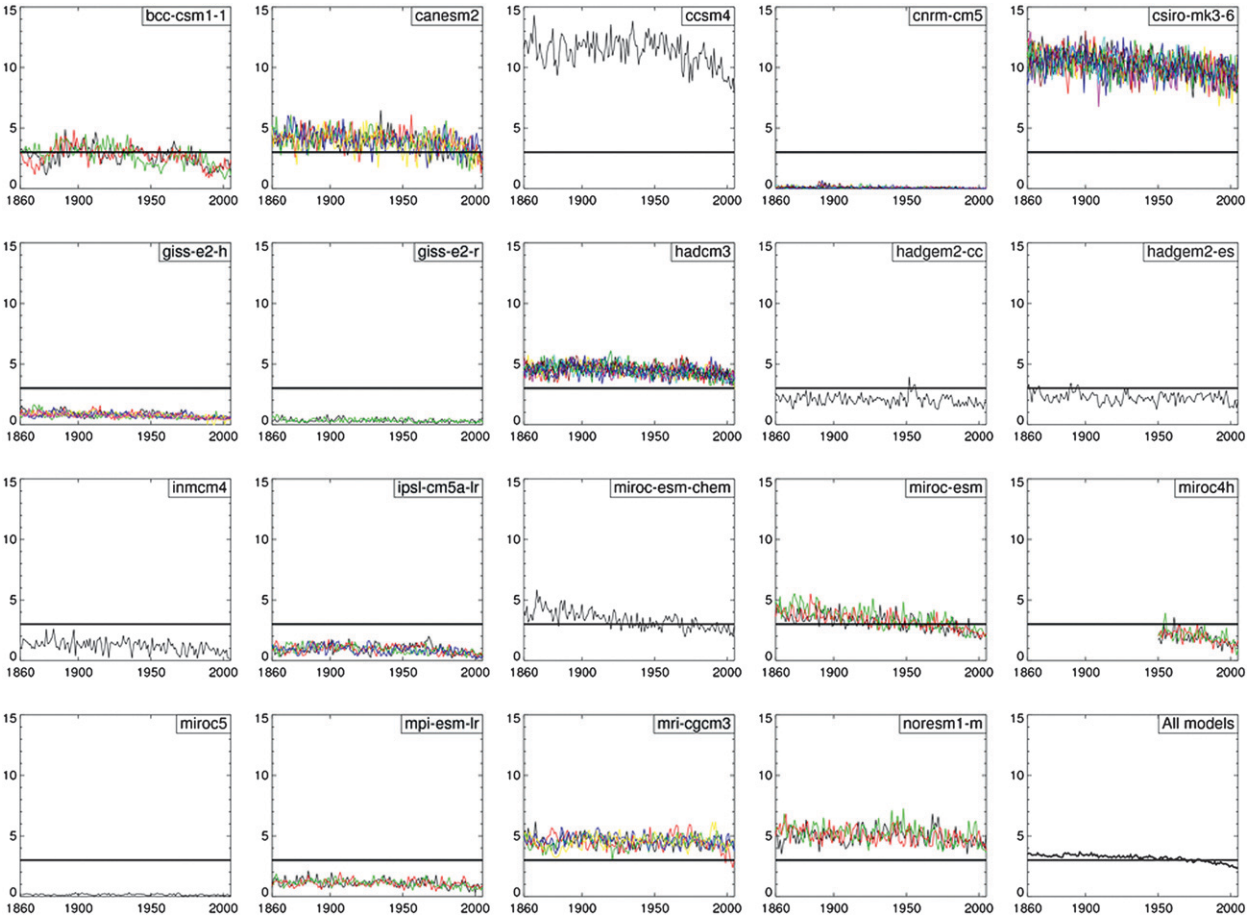

FIG. 3. The February SIE from 1860–2005 as simulated by the CMIP5 models. All ensemble members are plotted. The vertical scale is 10^6 km^2. The horizontal line indicates the mean (1979–2005) satellite extent of 3×10^6 km^2 for the month of February.

The absolute trends also have a large range (Fig. 1b), with the multimodel mean having the greatest absolute loss of ice of -0.40×10^6 km^2 decade^{-1} (-2.22% decade^{-1}) in September. This is very different from the largest absolute trend in the satellite data, which is an increase of 0.29×10^6 km^2 decade^{-1} in May. The largest differences between the absolute SIE model trends are found in October.

The February and March SIE trends in the satellite data are dominated by an increase (decrease) of ice in the Ross Sea (Amundsen–Bellingshausen Seas) and increases over the eastern Weddell Sea and, to a smaller extent, around the coast of East Antarctica. Figure 4 shows the spatial pattern of the trend in February sea ice concentration over 1979–2005 from the CMIP5 models and the satellite data. Clearly, the models with very little ice at the February minimum, such as MIROC5, GISS-E2-R, and CNRM, are not going to reproduce the spatial pattern of ice loss we see in the satellite data. However, even the models with a reasonable amount of sea ice in February, such as NorESM1-M and MRI-CGCM3, do not have the dipole of loss/increase that is seen in the satellite data between the Antarctic Peninsula and the Ross Sea. The models with very little sea ice in February only have significant amounts of ice over the western Weddell Sea and that decreases over 1979–2005.

We have a total of 70 model runs covering the period 1979–2005 from the 19 models listed in Table 1. These runs, which include three models that have 10 ensemble members, allow us to examine how the modeled trends vary due to simulated internal climate variability. The satellite data show that the annual mean SIE increased by 1.1% decade^{-1} over 1979–2005. Sixty-two runs had a negative trend in the annual mean SIE while eight had a positive trend, with seven having a trend that was larger than observed in the satellite data. If the models are doing a reasonable job at simulating the intrinsic variability of the climate system, then the results presented here suggest that there is approximately a 1 in 10 chance that the observed increase of ice extent is a result

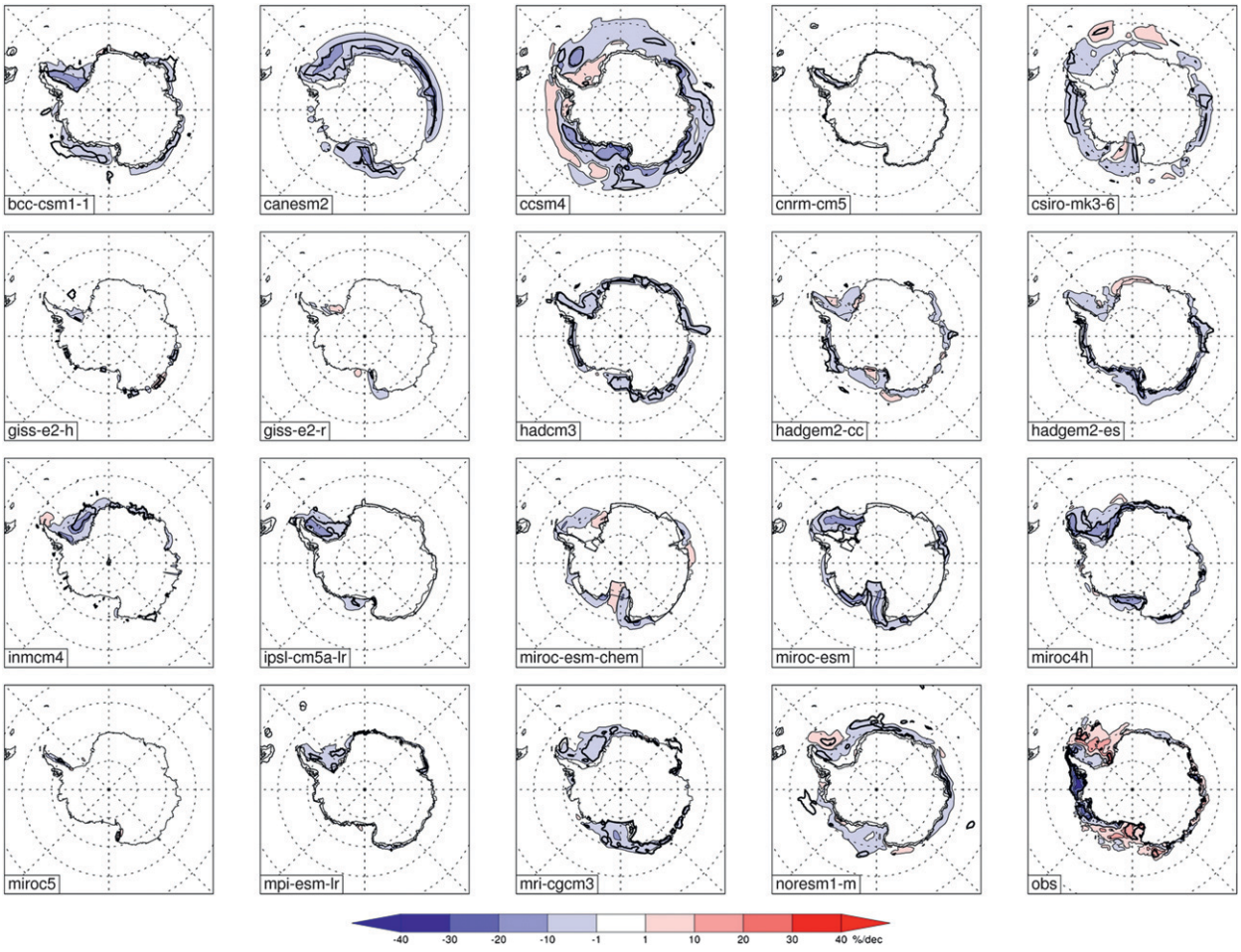

FIG. 4. The trend in February sea ice concentration over 1979–2005 from the CMIP5 models and the satellite data. For models with more than one ensemble member the mean of the ensemble members is shown.

of intrinsic variability. However, as indicated in Table 1, most of the models overestimate the variability of the annual mean SIE, thereby casting doubt on their value in helping us understand why the SIE has increased in the satellite era. Output from 10 ensemble members is available from the CSIRO-Mk3.6, CNRM-CM5, and HadCM3 models. All three models have a large variability in monthly trends between ensemble members (cf. Fig. 5 for CSIRO-Mk3.6). In all three models the largest difference between ensemble members is in late summer/early fall [SD 3.7% decade^{-1} for CSIRO-Mk3.6 (March), 3.6% decade^{-1} for HadCM3 (March), and 55.7% decade^{-1} for CNRM-CM5 (February)] and the smallest differences are close to the sea ice maximum in September. At the time of the SIE minimum in February/March there is still a large amount of shortwave radiation being received in the sea ice zone and the larger model spread in SIE trend at this time could well be a result of the amplifying effect of the ice–albedo feedback mechanism.

Given the interannual and lower-frequency variability that exists in SIE, it is interesting to examine multiple historical runs from a single model to see if the inconsistency between observed and modeled trends can be related to aliasing of natural variability. We focus on 10 ensemble members from the CSIRO-Mk3.6 model that have the same external forcing but different representations of intrinsic variability. All the CSIRO historical simulations are initialized with too much sea ice in February. The satellite era mean observed SIE in February is 3×10^6 km^2, with the extent in the 10 ensemble members varying from 9.3 to 9.7 $\times 10^6$ km^2. The ensemble members also simulate a wide range of trends in the February SIE, ranging from +4.98% decade^{-1} to −6.7% decade^{-1} (Fig. 5). It should also be noted that the CSIRO runs that had a positive trend in February SIE did not have the largest increase of ice in the Ross Sea as seen in the satellite data, but had ice increasing in all sectors around the continent.

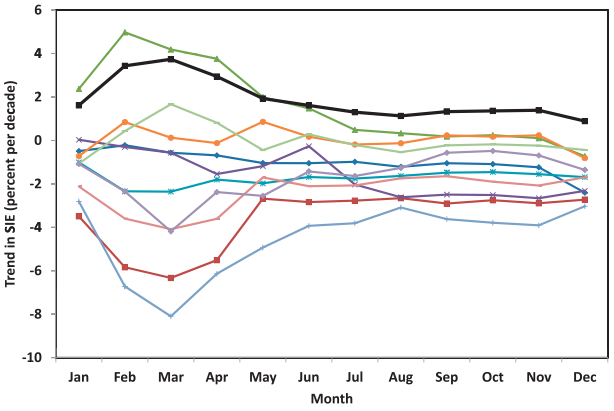

FIG. 5. Monthly trends of SIE of the 10 ensemble members of the CSIRO-Mk3.6 model over 1979–2005. The satellite SIEs are shown as a black line.

All 18 of the models that have historical runs starting in the mid-nineteenth century have a negative trend in February SIE over the entire length of the integrations, although not all the trends are significant. The mean of all the models' February SIE (Fig. 3) shows an accelerating decline over the last 40–50 years of the historical runs. This can be seen particularly clearly in the data for CCSM4, CanESM2, NorESM1-M, and IPSL-CM5A-LR. Such a trend is consistent with the increasing concentrations of CO_2 and other greenhouse gases. Although Fig. 3 shows interannual differences between model ensemble members (also see Table 1), there is a high degree of similarity between the trends across the different ensemble members, with the accelerated SIE decline in recent decades being a consistent feature.

In virtually all the models the SIE trends over 1979–2005 are a continuation of longer-term trends starting in the mid-twentieth century or earlier. However, it is instructive to examine the trends in the historical runs in comparison to the trends in the long control runs (Fig. 6). The majority of the control runs are for between 500 and 1000 years, and they give an indication of the long-term stability of the SIE when constant forcing is applied. Figure 6 shows that most of the runs have

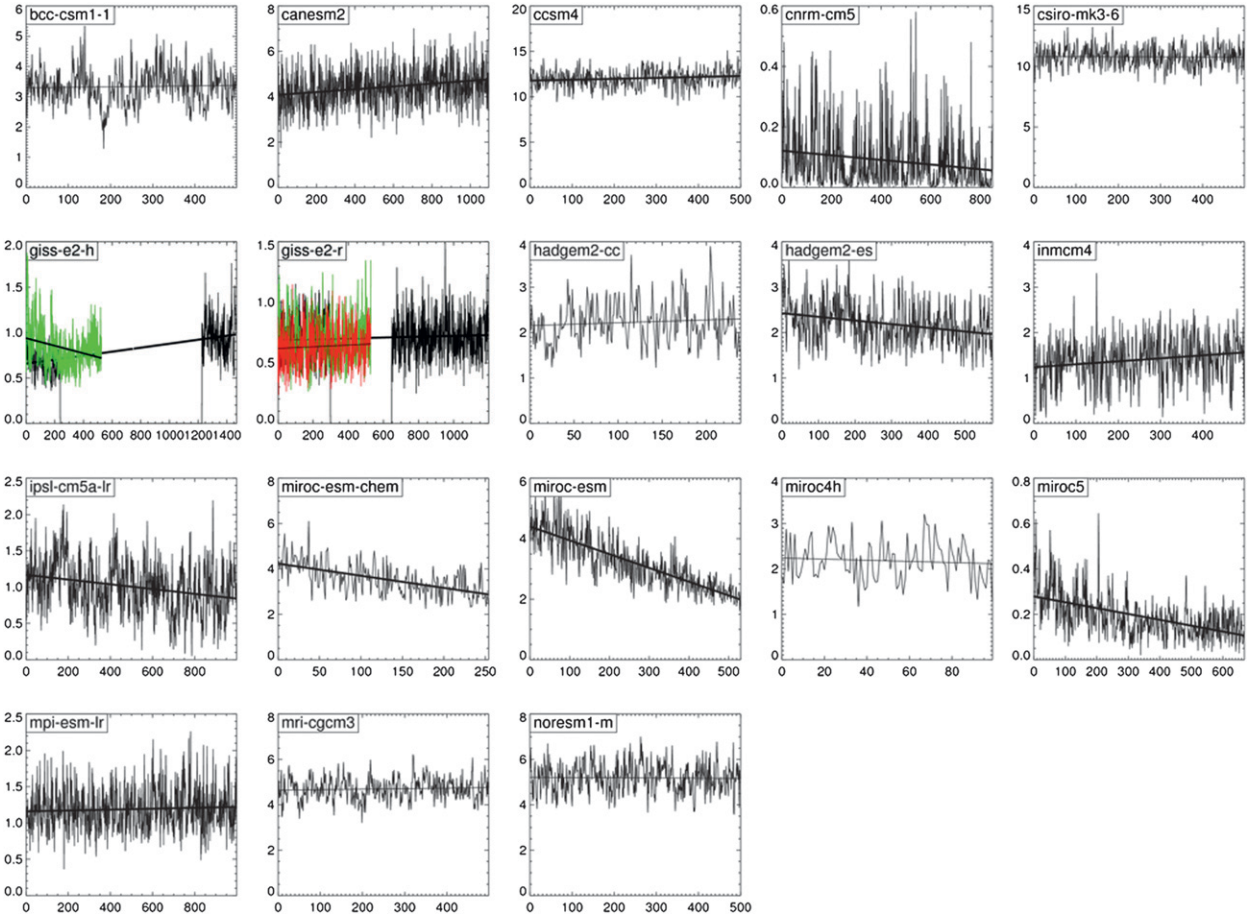

FIG. 6. The February SIE (10^6 km^2) in the control runs of the CMIP5 models along with the linear trends. The horizontal scale is in years. The vertical scales for the various models are different for clarity. For models where more than one control run was provided, the additional runs are shown in green and red. Note that the GISS-E2-H and GISS-E2-R models have gaps in the data provided.

drifts in the SIE throughout their whole time span despite the large interannual variability in the SIE, with 12 of the drifts being statistically significant (nine negative and three positive) and four not significant (here we have not considered the drifts in the GISS model control runs since there are gaps in the middle of the record). The largest negative drift is in the MIROC5 model, which has a decline of February SIE of -0.64% decade^{-1} over the 700 years of the run. All four of the MIROC runs have large decreases of February SIE that are in the range -0.39 to -0.64% decade^{-1}, but all the other models have drifts with an absolute magnitude of less than 0.15% decade^{-1}. Removing the long-term drifts from the 1979–2005 model SIE trends has little impact, as can be seen from corrected and uncorrected trends in Table 1. The large positive and negative SIE biases in the historical runs discussed earlier are apparent at the very start of the control runs, suggesting that these failings are established very early in the integrations.

5. Discussion and conclusions

We have shown that the CMIP5 models have a wide range of annual cycles of SIE and trends over recent decades, which is in broad agreement with the analysis of the CMIP3 data by Arzel et al. (2006). Although many of the models used in CMIP3 and CMIP5 are different, an equivalent of Fig. 3 produced from the available CMIP3 data (not shown) indicates that many of the SIE biases in the CMIP3 runs remain in CMIP5. Overall, the CMIP5 multimodel mean SIE for February over 1979–99 (Fig. 3) (2.79×10^6 km^2) is closer to the satellite data (2.9×10^6 km^2) than the comparable data for CMIP3 (3.47×10^6 km^2) [as in the study of Arzel et al. (2006), we have excluded the Flexible Global Ocean–Atmosphere–Land System Model, gridpoint version 1.0 (FGOALS-g1.0)] for the same period.

The mean SIE over 1860–2005 for the multimodel mean shown in Fig. 3 has no trend for approximately the first 50 years, but then declines at an accelerating rate for the remainder of the period. We have few sea ice extent observations for the period before 1979 so, given the lack of sea ice observations, it is not possible to verify the performance of the models over this period.

For the period of 1979 to 2005 the observations show an increase in SIE, with the greatest percentage change near the sea ice minimum. Clearly, many of the models have significant problems in their simulation of the sea ice minimum when the largest positive trend in SIE has been observed (cf. Fig. 1). This will make it very difficult for the models to correctly simulate an overall increase in SIE. However, even a model such as NORESM1-M, which has a good representation of the annual cycle of SIE, has an ice decrease in all its ensemble members. It could be that the processes responsible for the observed increase in SIE over the last 30 years are not being simulated correctly. Alternatively, if the recent increase in SIE is a result of natural variability, then we would not expect it to be reproduced in the majority of model runs.

A previous modeling study (Turner et al. 2009) suggested that the decrease of springtime stratospheric ozone was a factor in the recent increase in SIE. A criticism leveled at some of the IPCC AR4 (CMIP3) model runs was that they did not all have a representation of the ozone hole in their historical runs. However, the specification of the CMIP5 models requires the inclusion of a realistic decline in stratospheric ozone. Examination of the MSLP trends suggests that they are indeed showing atmospheric circulation changes consistent with ozone depletion. The failure to reproduce the observed increase in SIE may indicate that there are common failings in the representation of sea ice in the models or that a real trend in ocean conditions is behind the observed increase of sea ice. If, as suggested by Sigmond and Fyfe (2010), other factors beside the loss of stratospheric ozone are responsible for the increase in ice, then these are clearly not being represented by the CMIP5 models.

REFERENCES

Arzel, O., T. Fichefet, and H. Goosse, 2006: Sea ice evolution over the 20th and 21st centuries as simulated by current AOGCMs. *Ocean Modell.,* **12,** 401–415.

Comiso, J. C., and F. Nishio, 2008: Trends in the sea ice cover using enhanced and compatible AMSR-E, SSM/I and SMMR data. *J. Geophys. Res.,* **113,** C02S07, doi:10.1029/2007JC004257.

McLaren, A. J., and Coauthors, 2006: Evaluation of the sea ice simulation in a new coupled atmosphere–ocean climate model (HadGEM1). *J. Geophys. Res.,* **111,** C12014, doi:10.1029/2005JC003033.

Santer, B. D., T. M. L. Wigley, J. S. Boyle, D. J. Gaffen, J. J. Hnilo, D. Nychka, D. E. Parker, and K. E. Taylor, 2000: Statistical significance of trends and trend differences in layer-average atmospheric temperature time series. *J. Geophys. Res.,* **105** (D6), 7337–7356.

Screen, J. A., 2011: Sudden increase in Antarctic sea ice: Fact or artifact? *Geophys. Res. Lett.,* **38,** L13702, doi:10.1029/2011GL047553.

Sigmond, M., and J. C. Fyfe, 2010: Has the ozone hole contributed to increased Antarctic sea ice extent? *Geophys. Res. Lett.,* **37,** L18502, doi:10.1029/2010GL044301.

Song, H.-J., E. Choi, G.-H. Lim, Y. H. Kim, J.-S. Kug, and S.-W. Yeh, 2011: The central Pacific as the export region of the El Niño–Southern Oscillation sea surface temperature anomaly to Antarctic sea ice. *J. Geophys. Res.,* **116,** D21113, doi:10.1029/2011JD015645.

Stammerjohn, S., D. G. Martinson, R. C. Smith, X. Yuan, and D. Rind, 2008: Trends in Antarctic annual sea ice retreat and

advance and their relation to El Niño–Southern Oscillation and southern annular mode variability. *J. Geophys. Res.,* **113,** C03S90, doi:10.1029/2007JC004269.

Stroeve, J., M. M. Holland, W. Meier, T. Scambos, and M. C. Serreze, 2007: Arctic sea ice decline: Faster than forecast. *Geophys. Res. Lett.,* **34,** L09501, doi:10.1029/2007GL029703.

Turner, J., W. M. Connolley, D. Cresswell, and S. Harangozo, 2001: The simulation of Antarctic sea ice in the Hadley Centre climate model (HadCM3). *Ann. Glaciol.,* **33,** 585–591.

——, and Coauthors, 2009: Non-annular atmospheric circulation change induced by stratospheric ozone depletion and its role in the recent increase of Antarctic sea ice extent. *Geophys. Res. Lett.,* **36,** L08502, doi:10.1029/2009GL037524.

Zhang, J., 2007: Increasing Antarctic sea ice under warming atmospheric and oceanic conditions. *J. Climate,* **20,** 2515–2529.

Zwally, H. J., J. C. Comiso, C. L. Parkinson, D. J. Cavalieri, and P. Gloersen, 2002: Variability of Antarctic sea ice 1979–1998. *J. Geophys. Res.,* **107,** 3041, doi:10.1029/2000JC000733.